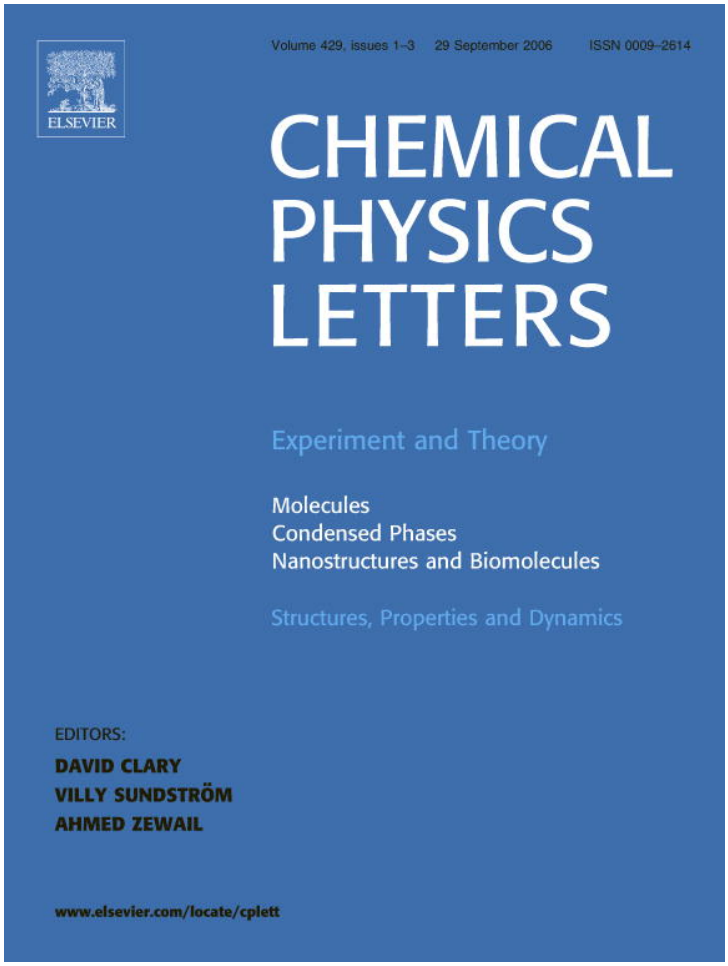

Available online at www.sciencedirect.com
ScienceDirect
Chemical Physics Letters 429 (2006) 276–281
CHEMICAL PHYSICS LETTERS
www.elsevier.com/locate/cplett

Fast transient absorption spectroscopy of the early events in photoexcited chiral benzophenone–naphthalene dyads

Raul Perez-Ruiz [a], Michiel Groeneveld [b], Ivo H.M. van Stokkum [c], Rosa Tormos [a], René M. Williams [b,*], Miguel A. Miranda [a,*]

[a] *Departamento de Química – Instituto de Tecnología Química UPV-CSIC, Universidad Politécnica de Valencia, Camino de Vera s/n, 46022 Valencia, Spain*
[b] *Molecular Photonics Group, Van't Hoff Institute for Molecular Sciences (HIMS), Universiteit van Amsterdam, Nieuwe Achtergracht 166, 1018 WV Amsterdam, The Netherlands*
[c] *Department of Physics and Astronomy, Vrije Universiteit, de Boelelaan 1081, 1081 HV Amsterdam, The Netherlands*

Received 10 March 2006; in final form 19 July 2006
Available online 1 August 2006

Abstract

Photoinduced intra-molecular energy transfer in two ketoprofen(KP)-naproxol(NPX) diastereomers proceeds via two pathways. Very fast singlet–triplet energy transfer ($k = 1.2 \times 10^{11}$ s^{-1}) from KP to NPX occurs for a small percentage (6%) and the major pathway is triplet–triplet energy transfer ($k \sim 3 \times 10^{9}$ s^{-1}). This was shown with femtosecond transient absorption spectroscopy and global and target analysis. Whereas the NPX triplet decay is strongly stereospecific (ratio of 1.6), the NPX triplet state formation for both dyads is very similar (ratio of 1 for the fast process and 1.2 for the slower process).

1. Introduction

Since the first report by Terenin and Ermolaev, benzophenone (BP)/naphthalene (NP) systems have been widely used as models to study inter- and intra-molecular singlet–singlet and triplet–triplet energy transfer processes [1–16]. Thus, Shizuka and coworkers have intensively investigated the sensitization of the NP triplet by BP, the behavior of the triplet-excited states of BP and NP and their interactions. The decay of the triplet state of NP was implied to occur by interaction with ground state BP through a loose sandwich-like structure [9–12]. This type of quenching, claimed different from electron or energy transfer, is inherent to the excited state interactions of BP and NP triplet states [4–12].

In covalently linked, flexible BP–NP dyads the decay of the NP triplet state (^{3}NP) will thus be governed by a folding process through which the ^{3}NP can π-interact with ground state BP. By using this concept we have shown that in chiral BP–NP systems stereospecific photophysical processes occur [16]. This was shown by monitoring the triplet state decay of two diastereomeric compounds (**1SS** and **2SR**, Chart 1) that consist of *S*-ketoprofen (KP) and *S* or *R*-naproxol (NPX). Unfortunately, the early photophysical events and potential stereoselective excited state effects in these dyads could not be monitored so far due to experimental limitations.

Here, we wish to report on femtosecond transient absorption spectroscopy of the early events in these two stereoisomeric compounds **1SS** and **2SR**, and the analysis thereof with spectrotemporal parameterization.

2. Experimental

Compounds **1SS** and **2SR** were synthesized by condensation of (2*S*)-2-(3-benzoylphenyl)-propanoic acid [(*S*)-ketoprofen, KP(*S*)] and (2*S*)- or (2*R*)-2-(6-methoxy-2-naphthyl)propan-1-ol [(*R*) or (*S*)-naproxol, NPX(*R*) or NPX(*S*)] following a previously reported procedure [16]. Briefly, (*R*) and (*S*)- naproxol were condensed with

* Corresponding authors.
E-mail addresses: williams@science.uva.nl (R.M. Williams), mmiranda@qim.upv.es (M.A. Miranda).

0009-2614/$ - see front matter © 2006 Elsevier B.V. All rights reserved.
doi:10.1016/j.cplett.2006.07.077

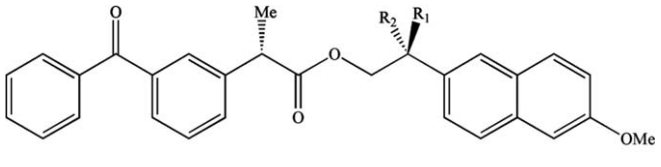

1SS: $R_1 = CH_3$; $R_2 = H$ (*S,S*)-KP-NPX
2SR: $R_1 = H$; $R_2 = CH_3$ (*S,R*)-KP-NPX

Chart 1. Molecular structures of dyads **1SS** and **2SR** consisting of (2*S*)-2-(3-benzoylphenyl)-propanoic acid [(*S*)-ketoprofen, KP(*S*)] and (2*S*)- or (2*R*)-2-(6-methoxy-2-naphthyl)propan-1-ol [(*R*) or (*S*)–naproxol, NPX(*R*) or NPX(*S*)].

(*S*)-Ketoprofen in the presence of dicyclohexylcarbodiimide and 4-(dimethylamino)pyridine, using dry methylene chloride as solvent. The two enantiomers of naproxol were obtained from (*R*)- or (*S*)-naproxen by reduction with $LiAlH_4$ in tetrahydrofuran. The obtained dyads were analyzed by ^1H and ^{13}C NMR; the spectra were identical to those reported in the literature.

Femtosecond transient absorption experiments were performed with a Spectra-Physics Hurricane Titanium: Sapphire regenerative amplifier system. The full spectrum setup was based on an optical parametric amplifier (Spectra-Physics OPA 800) as the pump. The residual fundamental light, from the pump OPA, was used for white light generation, which was detected with a CCD spectrograph (Ocean Optics). The OPA was used to generate excitation pulses at 355 nm. The laser output was typically 5 μJ pulse^{-1} (130 fs FWHM) with a repetition rate of 1 kHz. The samples were placed into cells of 2 mm path length (Hellma) and were stirred with a 'finger'. The concentrations of the compounds **1SS** and **2SR** were fixed by adjusting the absorbance of the solution at an arbitrary value between 0.8 and 1. The UV–Vis absorption spectra of the samples were measured before and after the laser experiments and were found to be virtually identical, thus ruling out a possible degradation or chemical change of the samples. All photophysical data reported here have a 5–10% error limit, unless indicated otherwise.

2.1. Global and target analysis

All time-gated spectra were collated in a matrix, which was globally fitted using a sequential kinetic scheme with increasing lifetimes. From this the lifetimes and the evolution associated difference spectra (EADS) were estimated. The instrument response function (IRF) is described by a GAUSSIAN shape, and the white light dispersion over the spectral range is modeled by a third order polynomial. With increasing lifetimes, and thus decreasing rates, the first EADS decays with the first lifetime and corresponds to the difference spectrum at time zero with an ideal infinitely small IRF. The second EADS is formed with the first lifetime and decays with the second lifetime, etc. The final EADS represents the difference spectrum of the longest living species. The error in the lifetimes obtained from the fitting procedure does not exceed 10%. EADS may not represent pure species, except for the final EADS, and they are interpreted as a weighted sum (with only positive contributions) of species-associated difference spectra (SADS). The quality of the fit was judged by inspection of the singular vectors of the matrix of residuals, which had to be structureless. Next, a kinetic scheme was used in the target analysis in combination with spectral assumptions to estimate microscopic rate constants and SADS. As a further refinement, to deal with fluctuations in the pump–probe overlap, we used the estimated SADS to fit the original data-matrices, with the help of a spectral model. Finally,

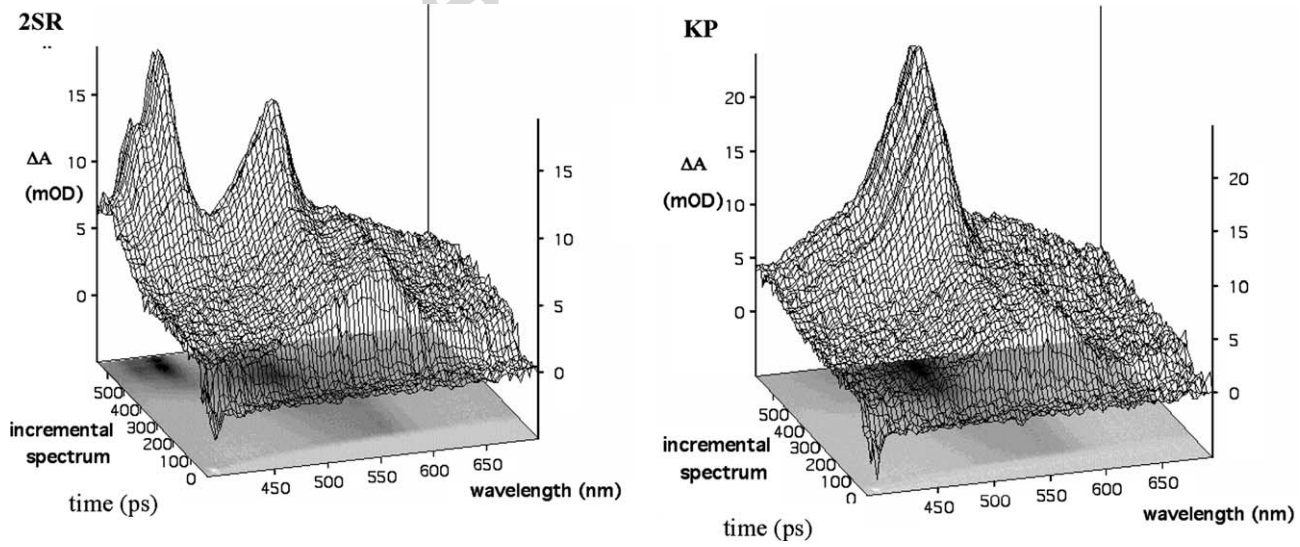

Fig. 1. 3D surface plots of the raw femtosecond transient absorption data of the dyad **2SR** (KP(*S*)-NPX(*R*)) and of KP in acetonitrile (2 mm cell-path, 5 μJ per pulse, 355 nm, 120 fs FWHM). Signal intensity is also projected on the *x*–*y* plane. The incremental time delay between the spectra is short (0.02 ps) at the start and longer (15 ps) at later times. At the earliest times, the chirp and some Raman scatter are observed. The conversion of the KP singlet into the KP triplet and subsequent NPX triplet formation is clear, for the dyad.

the thus estimated concentration profiles were again fitted with the kinetic scheme. A full description of the method has been given elsewhere [17,18].

3. Results and discussion

A 3D surface-plot representation of the femtosecond transient absorption spectra of **2SR** and of KP obtained using selective KP excitation at 355 nm is presented in Fig. 1. For **1SS** very similar data as for **2SR** were obtained. The excitation of NPX with 320 nm yielded a long-lived (ns) transient with a strong band at 440–450 nm and a shoulder at 550 nm. No signal was observed for NPX when 355 nm excitation was used. In Fig. 2 selected time-gated spectra at different delay times of **2SR** and KP are presented. Comparison of the two 3D surface-plots (Fig. 1) and the two sets of spectra in Fig. 2 clearly shows the overall conversion of the singlet excited state of KP (^{1}KP) absorbing at 570 nm, into ^{3}KP (530 nm) and the subsequent formation of ^{3}NPX (440 nm) in **2SR**. The similarity of the spectra of **2SR** and KP at early times is in accordance with selective KP excitation. A close inspection of the traces at 15 ps, however, shows that on this timescale already competing processes are occurring, as demonstrated by the small peak at 440 nm. A kinetic analysis of the data-matrices belonging to **1SS** and **2SR** is in agreement with this observation as the evolution associated difference spectra (EADS) belonging to the 8.5 ± 0.5 ps component clearly contain a small spectral contribution at 440 nm (see Fig. 3a). As this feature cannot be attributed to the ^{3}KP, it indicates a $6.1 \pm 0.4\%$ direct transfer of ^{1}KP to ^{3}NPX. This was observed for both **1SS** and **2SR**.

On the basis of these observations, a spectral and kinetic model was implemented in the analysis of the data-matrices

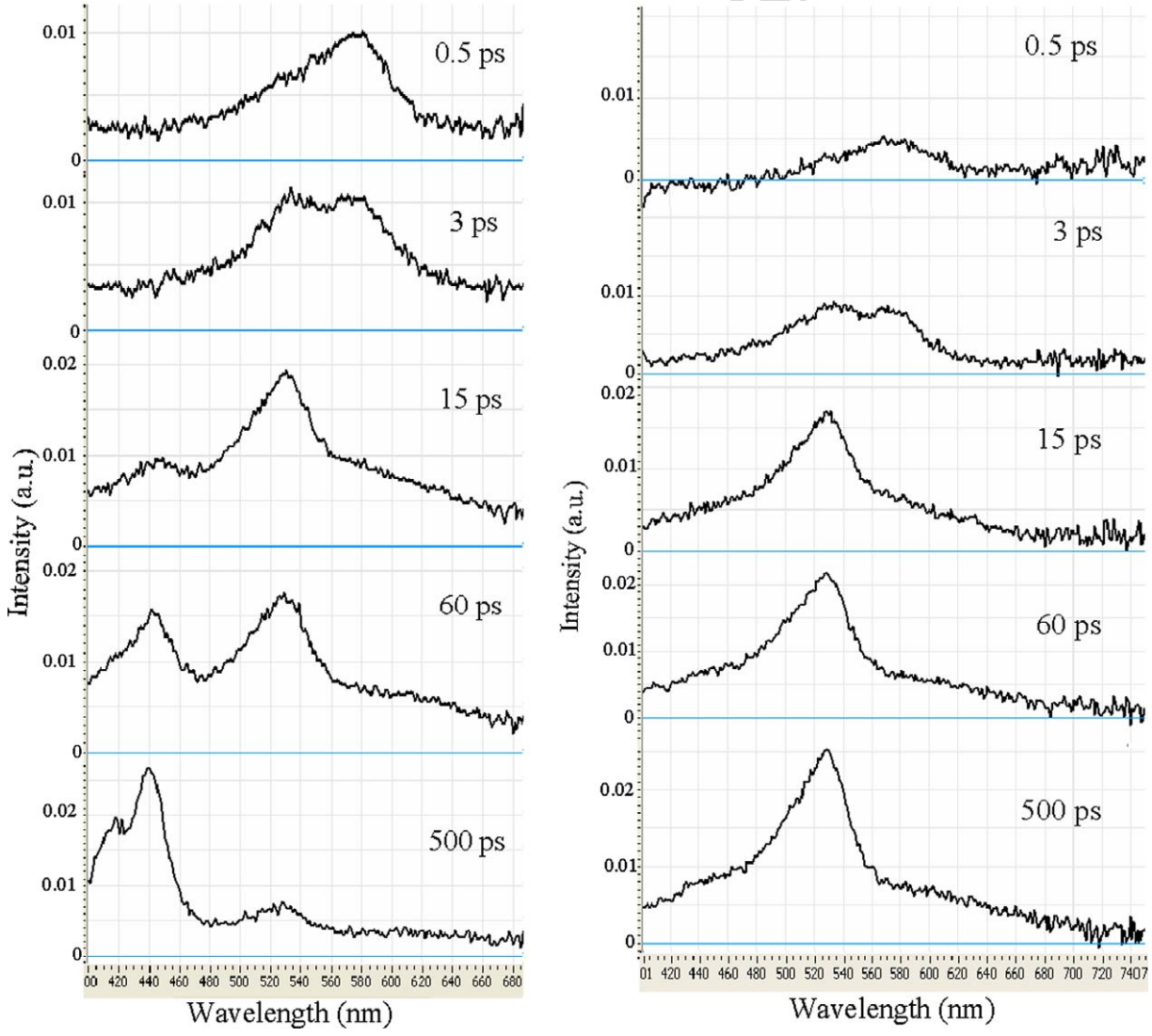

Fig. 2. Representation of selected transient absorption spectra of the dyad **2SR** (KP(*S*)–NPX(*R*)) (left) and of KP in acetonitrile (right) at different incremental time delays (time after pulsed (355 nm) pump-laser excitation) taken from the data of Fig. 1. Note that the difference between **2SR** and KP is already present in the 15 ps spectra.

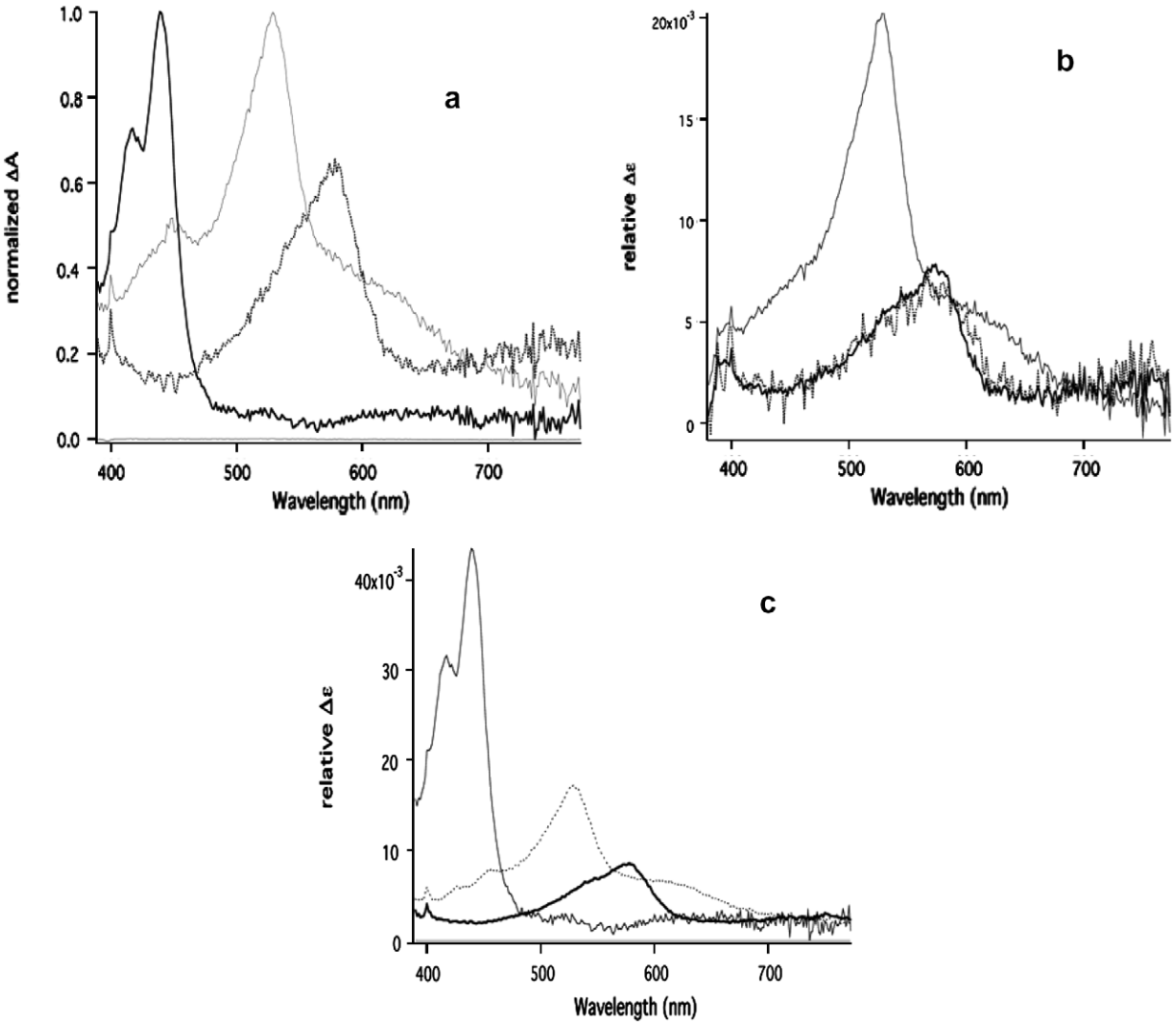

Fig. 3. (a) Normalized Evolution Associated Difference Spectra (EADS) of **2SR** showing the first fast component (dotted line), the second component (normal line) and the last component (thick line). The target analysis indicates that the 8.5 ps component contains ~6% NPX triplet state formation (i.e. compare the second component (normal line) to the triplet–triplet absorption of KP (normal line) in figure b). (b) Species Associated Difference Spectra (SADS) of ketoprofen (KP) obtained by spectrotemporal analysis. A 250 fs component (dotted line), the singlet–singlet absorption (11 ps, thick line) and the triplet–triplet absorption (normal line, infinite lifetime) are extracted. (c) Species Associated Difference Spectra (SADS) of **2SR** obtained by spectrotemporal analysis, on a relative extinction scale. The KP singlet–singlet absorption (8.5 ps, thick line) and the KP triplet–triplet absorption (dotted line) as well as the NPX triplet–triplet (normal line) absorption are extracted. The ratio of the extinction coefficient of the two triplet states is 3.

of KP, **1SS** and **2SR**. The results of this analysis yields species associated difference spectra (SADS) and kinetic parameters belonging to the different species.

The SADS of KP are represented in Fig. 3b. Apart from a Raman signal which follows the excitation pulse, also a 250 fs component was observed, with very similar spectral features as the $S_1 \rightarrow S_n$ absorption. We tentatively attribute this to intra-molecular vibrational relaxation within the singlet manifold (a similar 250 fs component was observed for all compounds. There are no distinctive solvent relaxation induced spectral shifts in the first two picoseconds). The $S_1 \rightarrow S_n$ absorption and the $T_1 \rightarrow T_n$ absorption on a relative ε-scale are represented in Fig. 3b. The band at 570 nm can easily be assigned to the ketoprofen singlet–singlet absorption, by comparison with the observations of Masuhara who applied the femtosecond grating spectroscopy technique to benzophenone [19]. The 530 nm band is attributed to the ketoprofen triplet–triplet absorption, which has been previously reported by e.g. Scaiano [20].

The SADS of **2SR** are represented in Fig. 3c. The similarity to KP of the first $S_1 \rightarrow S_n$ absorption and the $T_1 \rightarrow T_n$ absorption components is clear. The third component can be attributed to the ^{3}NPX. The transient absorption spectrum is very similar to that of naphthalene itself [16]. If we assume a 100% efficiency of triplet energy transfer we can estimate a ratio of the extinction coefficients of the triplet–triplet absorption of the KP and NPX triplet states of 3. This agrees well with the reported values [21] of the extinction coefficients of the triplet states of benzophenone and 2-methoxynaphthalene (7220 and 21 400).

The spectral and kinetic parameters indicate that the triplet state formation within the KP chromophore (8.5 ps) is accompanied by a ~6% fast transfer to the ^{3}NPX, and the ^{3}KP to the ^{3}NPX energy transfers occur with times of 380 ± 60 ps for **1SS** and 310 ± 30 ps for **2SR**. Thus the major triplet energy transfer rates are only slightly different. A comparison of the kinetic data at selected wavelengths with fits is represented in Fig. 4, as an illustration of the similarity of the dynamics of the fast processes in the two compounds.

In Fig. 5 the concentration profiles of the three species present in the excited state of **2SR** are represented. Whereas the figure clearly shows the conversion of the ^{1}KP into the ^{3}KP, it is accompanied by a small percentage of ^{3}NPX formation. Note that the concentration of ^{3}NPX is already substantial at 20 ps.

Based on these data, the major energy transfer rate constants, k_{en}, were calculated by using the following equation:

$$k_{en} = 1/\tau - 1/\tau_{ref} \quad (1)$$

where τ and τ_{ref} were the triplet lifetimes of the corresponding KP moiety in the diastereomers and in the reference compound KP ($\tau_{ref} = 1.3$ μs) [22], respectively. The triplet energy transfer rates are 1.2×10^{11} s^{-1} (minor component) and 3.2×10^9 s^{-1} for **1SS** and 2.6×10^9 s^{-1} for **2SR**. (The average value thus is $k \sim 3 \times 10^9$ s^{-1}.)

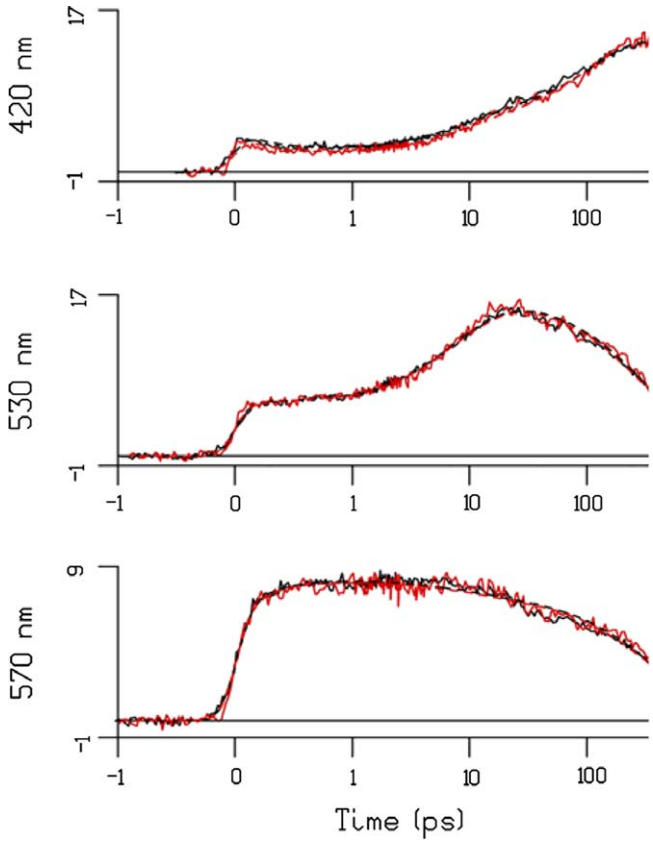

Fig. 4. A comparison of kinetic traces with fits of **1SS** (red) and **2SR** (black) at the three wavelengths corresponding to the singlet–singlet absorption of KP, the triplet–triplet absorption of KP and the triplet–triplet absorption of NPX. Clearly the kinetic traces are rather similar. Note that the time base is linear up to1 ps, and logarithmic thereafter. (For interpretation of the references to colour in this figure legend, the reader is referred to the web version of this article.)

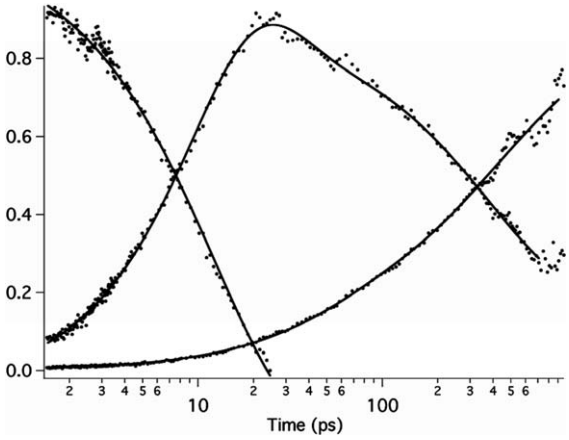

Fig. 5. The concentration profiles of the three species present in the excited state of **2SR**. The associated spectra are depicted in Fig. 3c. ^{1}KP converts into ^{3}KP and for a small part in the ^{3}NPX. ^{3}KP converts into ^{3}NPX, which lives very long.

As the Förster (coulombic) energy transfer mechanism is expected to have a negligible contribution due to the very low molar absorption coefficients of the ground state to triplet state transition which results in a very low spectral overlap integral, the appropriate mechanism must be Dexter-type (double electron exchange).

The singlet state of NPX is not formed by excitation as it does not absorb at 355 nm. Furthermore, its lifetime is much longer than the NPX triplet state formation observed in the dyad systems, implying the absence of (thermally activated) singlet–singlet energy transfer.

We can conclude that although the slow decay of the NPX triplet state in the dyads **1SS** and **2SR** is dominated by conformational folding effects that are strongly influenced by the stereo-centers present in the linking bridge, the NPX triplet state formation is governed by electronic effects. As the T–T energy transfer must proceed through a Dexter-type mechanism the electronic coupling in the two stereoisomers clearly is very similar. Surprisingly, a 6% component of fast (8.5 ps) energy transfer from singlet KP to the triplet of NPX is observed. Fast energy transfer processes that defy the spin selection rules have been observed before [23]. The major energy transfer pathway, however, is via the triplet state of KP and proceeds in 310 (**2SR**) and 380 ps (**1SS**).

Chart 2 summarizes the photophysical events that occur in the ketoprofen naproxol dyads: after 355 nm excitation a fast (250 fs) vibrational relaxation leads to the ketoprofen singlet state that decays in 8.5 ps. This decay mainly results in the ketoprofen triplet state formation by intersystem crossing but also small amount of singlet–triplet energy transfer from KP to NPX is observed. The triplet of KP then transfers its energy with τ's of 310 (**2SR**) and 380

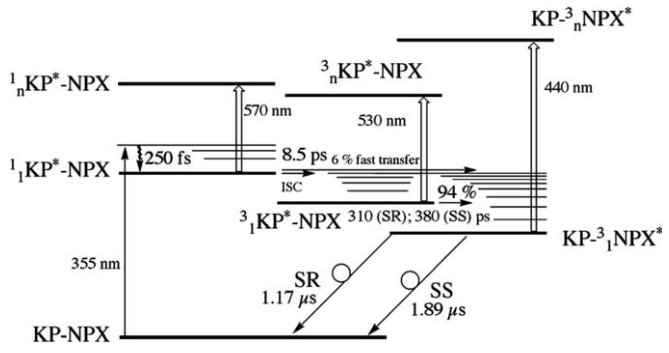

Chart 2. Energy level diagram indicating the processes occurring in the dyads **1SS** and **2SR**. Indicated are the multiplicity and localization of the excited state of the KP-NPX units, the excitation, excited state absorption (wide arrows) and the rates of the processes. The NPX triplet decay is strongly enantiospecific and proceeds via folding. The percentages are relative to the total excited state population.

(**1SS**) ps. The decay of the NPX triplet proceeds via a folding process that shows a strong stereospecificity.

Acknowledgement

The financial support from the MCYT (Grant No. CTQ2004–03811 and fellowship to Raúl Pérez-Ruiz), the Generalitat Valenciana (Grupos 03/82) and the Universidad Politécnica de Valencia (Grant No. 5648) is gratefully acknowledged. We thank NWO for the grant for the femtosecond equipment and the UvA for structural support. We would like to thank the referee of this Letter for the valuable suggestions, which were helpful in improving the work significantly.

References

[1] A. Terenin, V. Ermolaev, Trans. Faraday Soc. 52 (1956) 1042.
[2] W.M. Moore, M. Ketchum, J. Am. Chem. Soc. 84 (1962) 1368.
[3] G. Porter, F. Wilkinson, Trans. Faraday Soc. 57 (1961) 1686.
[4] A.A. Lamola, P.A. Leermakers, G.W. Byers, G.S. Hammond, J. Am. Chem. Soc. 87 (1965) 2322.
[5] R.W. Anderson Jr., R.M. Hochstrasser, H. Lutz, G.W. Scott, Chem. Phys. Lett. 32 (1975) 202.
[6] M.E. Sigman, G.L. Closs, J. Phys. Chem. 95 (1991) 5012.
[7] P.S. Engel, D.W. Horsey, J.N. Scholtz, T. Karatsu, A. Kitamura, J. Phys. Chem. 96 (1992) 7524.
[8] R.D. Fossum, M.A. Fox, J. Am. Chem. Soc. 97 (1997) 1197.
[9] H. Shizuka, Pure Appl. Chem. 69 (1997) 825.
[10] M. Yamaji, T. Tanaka, H. Shizuka, Chem. Lett. (1997) 19.
[11] T. Tanaka, M. Yamaji, H. Shizuka, J. Chem. Soc., Faraday Trans. 94 (1998) 7014.
[12] H. Shizuka, M. Yamaji, Bull. Chem. Soc. Jpn. 73 (2000) 267.
[13] W.G. McGimpsey, W.N. Samaniego, L. Chen, F. Wang, J. Phys. Chem. A 102 (1998) 8679.
[14] W.G. McGimpsey, L. Chen, R. Carraway, W.N. Samaniego, J. Phys. Chem. A 103 (1999) 6082.
[15] G. Bergamini, P. Ceroni, M. Maestri, V. Balzani, S. Lee, F. Vögtle, Photochem. Photobiol. Sci. 3 (2004) 898.
[16] M.C. Jiménez, S.-E. Stiriba, R. Tormos, J. Pérez-Prieto, M.A. Miranda, Photochem. Photobiol. Sci. 3 (2004) 36.
[17] I.H.M. van Stokkum, D.S. Larsen, R. van Grondelle, Biochim. Biophys. Acta 1657 (2004) 82.
[18] I.H.M. van Stokkum, R.H. Lozier, J. Phys. Chem. B 106 (2002) 3477.
[19] N. Tamai, T. Asahi, H. Masuhara, Chem. Phys. Lett. 198 (1992) 413.
[20] L.J. Martinez, J.C. Scaiano, J. Am. Chem. Soc. 119 (1997) 11066.
[21] S. Murov, I. Carmichael, G.L. Hug, Handbook of Photochemistry, 2nd ed., Marcel Dekker, New York, 1993.
[22] S. Encinas, N. Belmadoui, M.J. Climent, S. Gil, M.A. Miranda, Chem. Res. Toxicol. 17 (2004) 857.
[23] F. Lewitzka, H.G. Lohmannsroben, Zeit. Phys. Chem. Neue Folge 169 (1990) 203.